A Two-Stage Margin-Based Algorithm for Optimal Plug-in Electric Vehicles Scheduling

Francesco Baccino, *Student Member, IEEE,* Samuele Grillo, *Member, IEEE,*
Stefano Massucco, *Senior Member, IEEE,* and Federico Silvestro, *Member, IEEE*

I. Introduction

RECENTLY, considerable attention has been given to sustainable energy in various contexts. This rising collective awareness has induced a progressively growing need for changes, starting with the environmental impact of the economic strategies of countries and the design of new policies and paradigms for the management of cities and leading to attempts to reduce the carbon footprints of single human activities [1]–[3].

The pursuit of such objectives encourages the adoption of all electric solutions because of their better efficiency [4], [5]. One of the key aspects of this process is represented by transportation systems and, in particular, by road transport. Plug-in electric vehicles (PEVs) are part of this vision.

However, the growth in the electrical demand caused by the insertion of this new kind of loads (i.e., PEVs) may lead to a stressful usage of the power system distribution infrastructure. Many works have dealt with this problem that has to be managed by distribution system operators (DSOs) or other players [6]. For instance, in [7], the effects of PEV penetration on low voltage (LV) distribution networks were analyzed and compared in cases involving controlled and uncontrolled PEV loads. The proposed PEVs demand management system implements an agent approach, in which decisions are made on the basis of the value of a utility function. This paper was supported by a detailed model of the behavioral patterns that determine the traffic flow. In [8] and [9], the effects of PEVs recharge are analyzed on the basis of vehicle usage data. In the former problems on thermal rating of the feeder are detected as a consequence of PEVs connections and hosting capacity is estimated in an N and $N-1$ security scenario. In the latter, two different recharge strategies are analyzed and policies for peak-shifting are proposed. In [10] and [11], several different objective functions for PEV optimal charging were described, investigated, and tested, 24-h simulations performed to compare the outputs of the different strategies. In [12], a probabilistic approach to estimate users behavior is implemented to evaluate recharge profile in a 100% PEVs penetration scenario. In [13], the three-phase optimal power flow (OPF) framework described in [14] was applied, including PEV constraints in the problem. Four different objective functions were considered along a 24-h horizon. In [15], the impact of PEV uncontrolled recharge was assessed within a Monte Carlo framework that took into account probabilistic models of both traditional loads and PEVs. In [16], PEVs are included in a vehicle-to-grid (V2G) market framework and are used to provide services to the grid (such as up and down reserve). The schedule of PEVs charges is coordinated by a load aggregator in order to simultaneously satisfy end-users and network needs. The approach is focused on a transmission system level and does not include any technical constraint on distribution network. In [17], a decentralized control strategy is developed to optimally define the recharge schedule of PEVs using a noncooperative games approach to be implemented in a future electricity market and requiring an advanced communication infrastructure.

Starting from these results and experiences, the objective of this paper is to propose and validate an algorithm by which DSOs would easily manage PEVs' recharge. In this paper, an optimization algorithm for the definition of

Manuscript received February 19, 2014; revised July 23, 2014 and November 3, 2014; accepted December 6, 2014. Date of publication December 30, 2014; date of current version February 16, 2015.

F. Baccino, S. Massucco, and F. Silvestro are with the Department of Electrical, Electronic, and Telecommunication Engineering and Naval Architecture, Università degli Studi di Genova, Genova I-16145, Italy.

S. Grillo is with the Dipartimento di Elettronica, Informazione e Bioingegneria, Politecnico di Milano, Milan 20133, Italy (e-mail: samuele.grillo@polimi.it).

Color versions of one or more of the figures in this paper are available online.

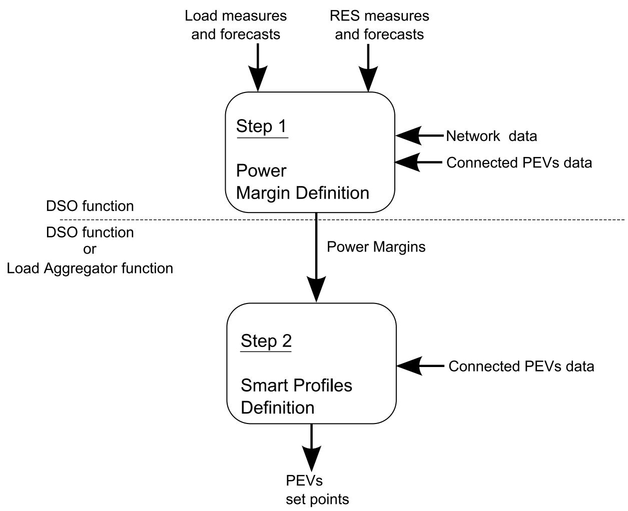

Fig. 1. Two-stage algorithm conceptual flowchart.

the optimal recharge profiles of PEVs is developed. The algorithm is designed to be fast and to fully exploit the existing communication and electrical infrastructure. The proposed algorithm has been tested using the CIGRÉ European low voltage benchmark network [18].

This paper is organized as follows. Section II is dedicated to the formal definition of the algorithm, along with a description of the operating condition framework for which the algorithm was designed. Section III describes the case study used for the test and validation of the proposed algorithm. Section IV is devoted to the presentation of the results. The conclusion is drawn in Section V.

II. Algorithm Description

The main idea of the optimization algorithm is that every user who connects his/her PEV to a charging station (both a private and a "public" one) can automatically receive a recharge profile optimized in terms of both grid security and user preference (e.g., charge duration).

The algorithm, as depicted in Fig. 1, can be divided into two parts: 1) power margin definition; and 2) smart profiles definition. The former, which must be carried out by the distribution system operator (DSO), involves the use of an OPF algorithm in order to define the bounds to which each PEV is subject during the assigned recharge time—by either the user, a PEV-recharge-service operator, the DSO itself or any other subject in charge. Once these limits are defined the latter phase, which can be performed either by the DSO itself or by an independent service provider (e.g., a load aggregator), finds the optimal recharge profile for each connected PEV. Each of these profiles is constrained by the bounds imposed by the previous optimization (i.e., the power margin definition) and by the bounds imposed by the user preferences (e.g., the amount of energy that should be provided, recharge time, etc.).

A. Power Margin Definition

This first step aims at the definition of the maximum power that each PEV can drain from the grid without exceeding the technical constraints of the network, i.e., busbar voltages and line currents [19]. In order to obtain this result, an OPF algorithm has been used. Each PEV is modeled as a "negative generator" (i.e., dispatchable load) and the associated cost function is suitably designed so that OPF algorithm obtains, by means of a minimization, the desired results (i.e., maximum limit values).

OPF algorithm receives as input data concerns the following:

1) network topology;
2) electrical loads;
3) renewable energy sources (RES) production;
4) PEVs connection node;
5) PEVs recharge time;
6) PEVs recharge energy.

After performing the optimization, returns, for every time interval, the maximum power that each PEV can drain from the grid. It is worth noting that data concerning loads and RESs production are forecast values. Many works have presented different approaches for RESs and load modeling, which can be used as a starting point to build a managed scheduling of PEVs [20], [21].

The power injection $P_i(t)$ of the ith PEV at tth time step is always negative

$$-P_i^{\max} \le P_i(t) \le 0. \tag{1}$$

OPF algorithm computes the optimal negative or positive power injections for every dispatchable load and every dispatchable generator respectively, minimizing an objective function which, in general, depends on active and reactive powers

$$\hat{J}(t) = \min_{\boldsymbol{\vartheta},\boldsymbol{V},\boldsymbol{P},\boldsymbol{Q}} \left(\sum_{k=1}^{N_{\text{gen}}} f_{\text{gen}}^k (P_k(t), Q_k(t)) + \sum_{i=1}^{N_{\text{PEV}}} f_{\text{PEV}}^i (P_i(t), Q_i(t)) \right) \tag{2}$$

where $\boldsymbol{V}$ is the vector of the magnitude of the voltage phasor of the busses, $\boldsymbol{\vartheta}$ is the vector of the angle of the voltage phasor of the busses, $\boldsymbol{P}$ is the vector of active power injections, $\boldsymbol{Q}$ is the vector of reactive power injections, N_{gen} is the number of dispatchable generators, and N_{PEV} is the total number of PEVs. In this paper, without lacking of generality, the only "dispatchable generator" in the LV distribution network is the main supply derived from the medium voltage feeder and the associated cost is set to zero for both active and reactive power. Moreover, PEVs cost function is assumed to have no dependence on the reactive power consumption—PEVs absorb power at unit power factor—and it is chosen proportional to the power drained by each PEV

$$f_{\text{PEV}}^i (P_i(t), Q_i(t)) = kP_i(t) = -k|P_i(t)|. \tag{3}$$

In this way, the minimization of the objective function of the OPF algorithm implies the maximization of the power absorbed by PEVs

$$\begin{aligned}\hat{J}(t) &= \min_{\boldsymbol{\vartheta},\boldsymbol{V},\boldsymbol{P},\boldsymbol{Q}} \sum_{i=1}^{N_{\text{PEV}}} f_P^i(P_i(t)) = \min_{\boldsymbol{\vartheta},\boldsymbol{V},\boldsymbol{P},\boldsymbol{Q}} \sum_{i=1}^{N_{\text{PEV}}} kP_i(t) \\ &= \min_{\boldsymbol{\vartheta},\boldsymbol{V},\boldsymbol{P},\boldsymbol{Q}} \sum_{i=1}^{N_{\text{PEV}}} -k|P_i(t)| = k \max_{\boldsymbol{\vartheta},\boldsymbol{V},\boldsymbol{P},\boldsymbol{Q}} \left(\sum_{i=1}^{N_{\text{PEV}}} |P_i(t)| \right).\end{aligned} \tag{4}$$

B. Smart Profiles Definition

Once the OPF establishes the maximum power that each PEV can absorb within the technical constraints—i.e., $\hat{P}_i(t) = \arg \hat{J}(t)$—a linear optimization is performed aiming at satisfying the users' needs (basically recharge time and energy) in an economic and sustainable way.

Let $\boldsymbol{x}$ be the vector of the power values which define the smart charge profiles for each PEV

$$\boldsymbol{x} = \begin{bmatrix} \boldsymbol{x}_1 \\ \boldsymbol{x}_2 \\ \vdots \\ \boldsymbol{x}_{N_k} \end{bmatrix} \tag{5}$$

where N_k is the number of PEVs connected in the interval $[t_k,\ t_{k+\max_i(T_i^{\mathrm{chg}})}]$—being T_i^{chg} the recharge time for the ith PEV—and each vector $\boldsymbol{x}_i$ (which defines the smart charge profile for the ith PEV) has T_i^{chg} elements. Each element of the vector $\boldsymbol{x}_i$ has to respect the constraint on power consumption, i.e., $\hat{P}_i(t)$, imposed by the OPF at every time interval. Using the matrix formalism this results in

$$\boldsymbol{A}_i \boldsymbol{x}_i \leq \hat{\boldsymbol{P}}_i \tag{6}$$

or, in a more explicit way

$$\begin{bmatrix} 1 & 0 & \cdots & 0 \\ 0 & 1 & \cdots & 0 \\ \vdots & \vdots & \ddots & \vdots \\ 0 & 0 & \cdots & 1 \end{bmatrix} \begin{bmatrix} x_i(t_k) \\ \vdots \\ x_i(t_{k+T_i^{\mathrm{chg}}}) \end{bmatrix} \leq \begin{bmatrix} \hat{P}_i(t_k) \\ \vdots \\ \hat{P}_i(t_{k+T_i^{\mathrm{chg}}}) \end{bmatrix} \tag{7}$$

where $\boldsymbol{A}_i$ is a unit matrix of size T_i^{chg}. If more than one PEV at a time is considered, inequality (6) becomes

$$\boldsymbol{A}\boldsymbol{x} \leq \hat{\boldsymbol{P}} \tag{8}$$

where the matrix $\boldsymbol{A}$ is a unit matrix of size $\sum_{i=1}^{N_k} T_i^{\mathrm{chg}}$ made up of the different matrices $\boldsymbol{A}_i$

$$\begin{bmatrix} \boldsymbol{A}_1 & \boldsymbol{0} & \cdots & \boldsymbol{0} \\ \boldsymbol{0} & \boldsymbol{A}_2 & \cdots & \boldsymbol{0} \\ \vdots & \vdots & \ddots & \vdots \\ \boldsymbol{0} & \boldsymbol{0} & \cdots & \boldsymbol{A}_{N_i} \end{bmatrix} \begin{bmatrix} \boldsymbol{x}_1 \\ \vdots \\ \boldsymbol{x}_{N_i} \end{bmatrix} \leq \begin{bmatrix} \hat{\boldsymbol{P}}_1 \\ \vdots \\ \hat{\boldsymbol{P}}_{N_k} \end{bmatrix}. \tag{9}$$

The elements of the vectors $\boldsymbol{x}_i$ have also to fulfill an energy requirement: the sum of the energies absorbed during the recharge time has to be equal to the energy E_i^{chg} requested by the user

$$k_E \boldsymbol{A}_i^{\mathrm{eq}} \boldsymbol{x}_i = E_i^{chg} \tag{10}$$

$$k_E\,[\,1\,1 \cdots 1\,] \begin{bmatrix} x_i(t_k) \\ \vdots \\ x_i(t_{k+T_i^{\mathrm{chg}}}) \end{bmatrix} = E_i^{\mathrm{chg}} \tag{11}$$

where $\boldsymbol{A}_i^{\mathrm{eq}}$ is a row vector constituted by as many "1" as the number T_i^{chg} and k_E is a constant whose value depends on the considered time interval (e.g., if quarter-hour time intervals are considered—during which power consumption is assumed to be constant—k_E has to be equal to 0.25 to obtain energy values expressed in kWh). If more than one PEV at a time is considered (10) becomes

$$k_E \boldsymbol{A}^{\mathrm{eq}} \boldsymbol{x} = \boldsymbol{E}^{\mathrm{chg}} \tag{12}$$

where $\boldsymbol{A}^{\mathrm{eq}}$ is a matrix with $\sum_{i=1}^{N_k} T_i^{\mathrm{chg}}$ columns and N_k rows, made up of the matrices $\boldsymbol{A}_i^{\mathrm{eq}}$

$$k_E \begin{bmatrix} \boldsymbol{A}_1^{\mathrm{eq}} & \boldsymbol{0} & \cdots & \boldsymbol{0} \\ \boldsymbol{0} & \boldsymbol{A}_2^{\mathrm{eq}} & \cdots & \boldsymbol{0} \\ \vdots & \vdots & \ddots & \vdots \\ \boldsymbol{0} & \boldsymbol{0} & \cdots & \boldsymbol{A}_{N_k}^{\mathrm{eq}} \end{bmatrix} \begin{bmatrix} \boldsymbol{x}_1 \\ \vdots \\ \boldsymbol{x}_{N_i} \end{bmatrix} \leq \begin{bmatrix} E_1^{\mathrm{chg}} \\ \vdots \\ E_{N_k}^{\mathrm{chg}} \end{bmatrix}. \tag{13}$$

Finally, the upper and lower bound limits have to be considered. Each element $x_i(t)$ cannot be either lower than a minimum value (zero, since in this scenario V2G is not allowed) or higher than the power limits defined upon contractual agreement between DSO and vehicle owner

$$0 \leq x_i(t_k) \leq P_i^{\max}. \tag{14}$$

The optimization aims at the minimization of a cost function within a subspace defined by the aforementioned constraints. The cost function J depends on the smart charge profiles (i.e., the unknown variables) and its simpler (and linear) formulation can be expressed as

$$J = \min_{\boldsymbol{x}} \boldsymbol{f}^{\mathrm{T}} \boldsymbol{x} \tag{15a}$$

s.t.

$$\boldsymbol{A}\boldsymbol{x} \leq \hat{\boldsymbol{P}} \tag{15b}$$

$$k_E \boldsymbol{A}^{\mathrm{eq}} \boldsymbol{x} = \boldsymbol{E}^{\mathrm{chg}} \tag{15c}$$

$$\boldsymbol{0} \leq \boldsymbol{x} \left(\leq \boldsymbol{P}^{\max}\right). \tag{15d}$$

If $\boldsymbol{f}$ is a column vector of -1, (15a) corresponds to maximize the total energy supplied to the PEVs. Other formulations of the cost function may easily consider the dependence on other variables, such as the cost of energy in the different moments of the day or CO_2 production. It is worth noting that constraint (15d) may be reduced by omitting the part within brackets, since the maximum value for each PEV and for every time interval is already defined in constraint (15b).

C. Benchmark Recharge Profile

In order to comparatively evaluate the benefits related to the implementation of a smart charge algorithm a nonoptimal recharge algorithm is needed. The term "nonoptimal charge" usually refers to a charge at the maximum contractual power lasting as long as the battery has been fully charged (i.e., constant-power recharge in [9]). Comparing this "traditional" nonoptimal charge with the proposed charging strategy would be somewhat unfair because the recharge duration would be significantly different in the two cases. In addition to that, the energy requested by each PEV would be constrained to integer multiples of 3.3 kW × 0.25 h = 0.825 kWh, which approximately correspond to a 5 km range. This would result in an excessive homogeneity of the daily traveling distances and consequently in a homogenization of the energy requests. Thus, the nonoptimal charge profile is defined by dividing the requested energy by the recharge time, the result of this ratio

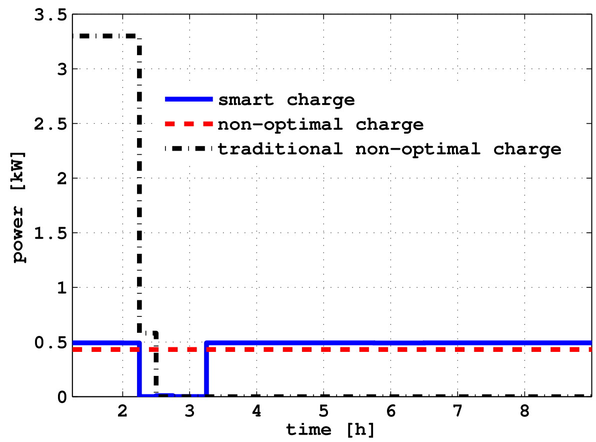

Fig. 2. Comparison among a smart charge (solid blue line), a nonoptimal charge as considered in this paper (dashed red line), and a traditional nonoptimal charge (dash-dotted black line).

being the power that the PEV constantly demands during the recharge time (i.e., constant-time recharge in [9]).

It is worth mentioning that, should the proposed optimal charging strategy perform better than the aforementioned nonoptimal charge, it would also perform better than the "traditional" nonoptimal charge . The three different recharge profiles are compared in Fig. 2.

A marginal note concerns the 3.3 kW value. It has been chosen because it is the minimum (and most common) size for Italian private power supply contracts.

III. Case Study

Due to the stochastic nature of the phenomena under examination (private cars travel habits and load profiles), the long-term effects of the algorithm and the impact of not completely reliable forecasts will be investigated in subsequent works with Monte Carlo simulations. In this paper, we focus on describing the algorithm and illustrating its operation in a case study simulation.

A. Benchmark Distribution Network

The test network used for the simulations is the residential feeder of the CIGRÉ LV benchmark network [18], the single line diagram of which is depicted in Fig. 3. The feeder is made up of a MV/LV transformer, 18 lines and 19 nodes. There are five load nodes (i.e., R11, R15, R16, R17, and R18) to which PEVs connect for recharge. For more detailed information concerning network parameters and configuration refer to [18] and, for analyses of PEVs impact on LV networks and its possible use refer to [22].

B. PEV Connections and Requests

The number of PEVs in the network is chosen equal to 300. This figure is relatively high and addresses a situation in which the PEVs market penetration is extremely consistent, as if almost all private vehicles were PEVs. This assumption is made to provide clearer evidences of the algorithm operation.

The characteristics of the PEVs simulated in this paper correspond to an average city car. The most significant data

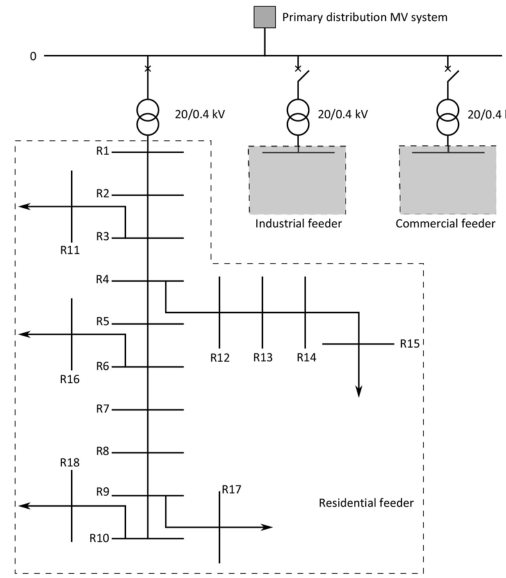

Fig. 3. Single line diagram of the residential feeder of the CIGRÉ LV benchmark network.

TABLE I
General Parameters of PEVs Used for Building the Simulation Scenario

Symbol	Description	Value	
$\mathrm{range}_{\max}$	maximum range	150.0	km
η	tank-to-wheel efficiency	0.15	kWh/km
η_{chg}	recharge efficiency	0.9	—
$P^{\max}$	maximum recharge power	3.3	kW

are listed in Table I. These data have been used to build the simulation scenario and to define the energy request of each PEV. Starting from the daily mileage—$\mathrm{range}_{\max}$ is the upper bound—the energy request is calculated using the tank-to-wheel efficiency. This energy request is increased by $1/\eta_{\mathrm{chg}}$ to take into account losses in power conversion stages.

The times of connection and the energy requests are selected according to indications derived by regional mobility surveys [23]. These data are processed in order to take into account the residential nature of the studied network, thus the connections are more numerous during the lunch-break time and of course in the evening starting from 6 P.M. The number of PEVs which connect to the network in each quarter of an hour is depicted in Fig. 4. The energy request is equal to the daily consumption (deducted from the daily mileage) and there is a consistency check that verifies the feasibility of the recharge within the desired time taking into account the charge power limit and efficiency. It is also assumed that the customers can select one of three possible recharge slots: 3, 5, or 8 h. Shorter durations are preferred during the day while longer ones are more common in the evening connections. Finally, the node of connection is randomly selected.

In this paper, OPF and power flow calculations are performed with MATPOWER [24]. The proposed methodology can be easily implemented using other tools that allow to customize the OPF objective function (Step 1 of the

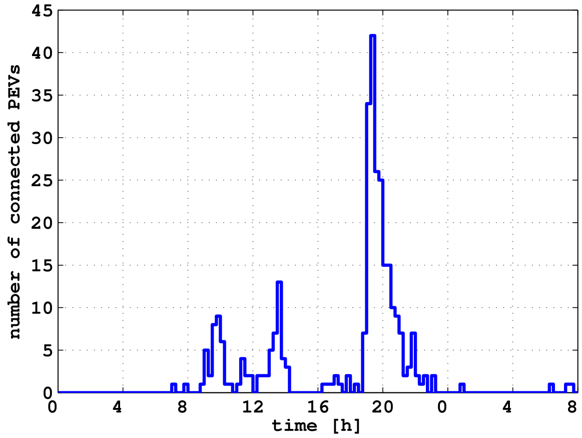

Fig. 4. Number of PEVs which connect to the network in each time interval.

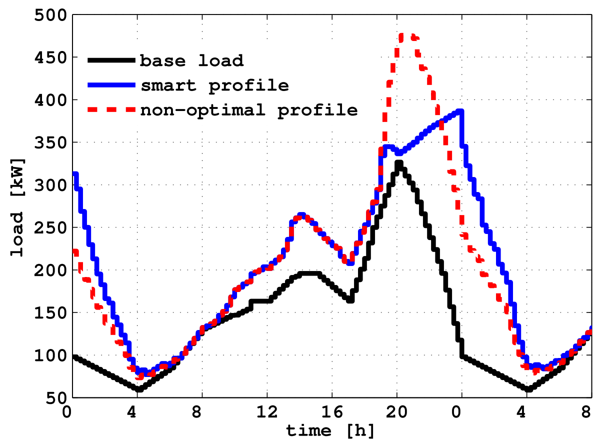

Fig. 5. Feeder load profile. Base case (solid black line), optimal recharge (solid blue line), and nonoptimal recharge (dotted red line).

proposed algorithm) and solve a linear optimization problem (Step 2). As mentioned before, this paper does not investigate different and new power flow and OPF solving algorithms. It is instead about proofing how tools already commercially available to DSOs, load aggregators and other stakeholders can be efficiently used to address the issue of PEV smart charge.

IV. Results

Simulation results related to a full day extended analysis are reported in this section. The optimal and nonoptimal recharge strategy effects on load profiles, bus voltages, and branch element load factors are compared and discussed.

The whole algorithm runs in few seconds (average value of 2.22 s on a normal desktop) with simultaneous connections of nearly 45 PEVs. It is also worth noting that the proposed algorithm can be easily implemented in order to run in parallel (i.e., one task for every primary distribution station) and/or in a distributed control framework. Therefore, this procedure is suitable to be deployed on a real-time on-line application.

The active power profile at the LV side of the distribution transformer is depicted in Fig. 5: without PEV (solid black line) and with PEV in the two cases, optimal recharge (solid blue line) and nonoptimal recharge (dotted red line).

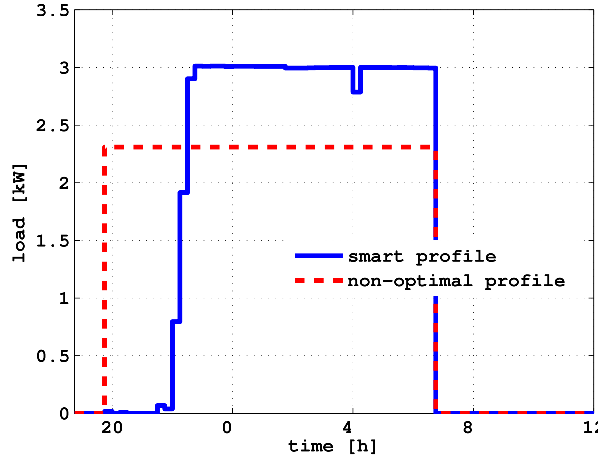

Fig. 6. Maximum PEV recharge profiles: optimal recharge (solid blue line) and nonoptimal recharge (dotted red line).

Fig. 5 clearly shows that the algorithm limits the power consumption during the evening hours, when the LV distribution peak occurs. Thus, PEVs are forced to complete the recharge later in the night. This result can be seen as a combination of "valley-filling" and "peak-shifting" behaviors.

It is worth noting that the objective function, as defined in (15a), maximizes energy absorption in every time interval without violating network constraints. In this way, among customers' possible needs top priority is given to time recharge. This fact means that even more significant changes in the load shape could be obtained inserting in the objective function other—typically price-based—constraints.

Fig. 6 shows a comparison between smart and nonoptimal recharge profiles of the PEV which requires the maximum energy during the simulation. These curves depict how the algorithm acts on a single PEV and how the peak shift is achieved.

Figs. 7 and 8 show branch elements load factors and voltage profiles. In both figures right-hand-side plots are the results obtained when the smart charge algorithm is active, while left-hand-side plots show the same quantities when PEVs connect and charge without any control.

It can be noticed that in the present test network capacity limits of the cables are the most stringent constraints. In fact, while Fig. 8(a) shows voltage profiles in all load buses are within the limits (i.e., $\pm 10\%$), Fig. 7(a) clearly shows that the first lines after the MV/LV transformer are overloaded during peak hours if no corrective action is performed. The proposed smart charge algorithm, as depicted in Fig. 7(b), reduces load factors below the limits.

Obviously, the smart charge algorithm positively affects the voltage profiles as well. In Fig. 9, the voltage profile of the bus located at the bottom of the feeder, i.e., the more exposed to under voltage problems, is reported. It can be seen how the smart charge algorithm makes the voltage profile smoother and avoids the deep voltage sag that corresponds to the overlapping of the evening peak with the PEVs connection peak.

A final remark can be done on the overall characteristics of the simulations. As shown in Table II, each PEV recharges

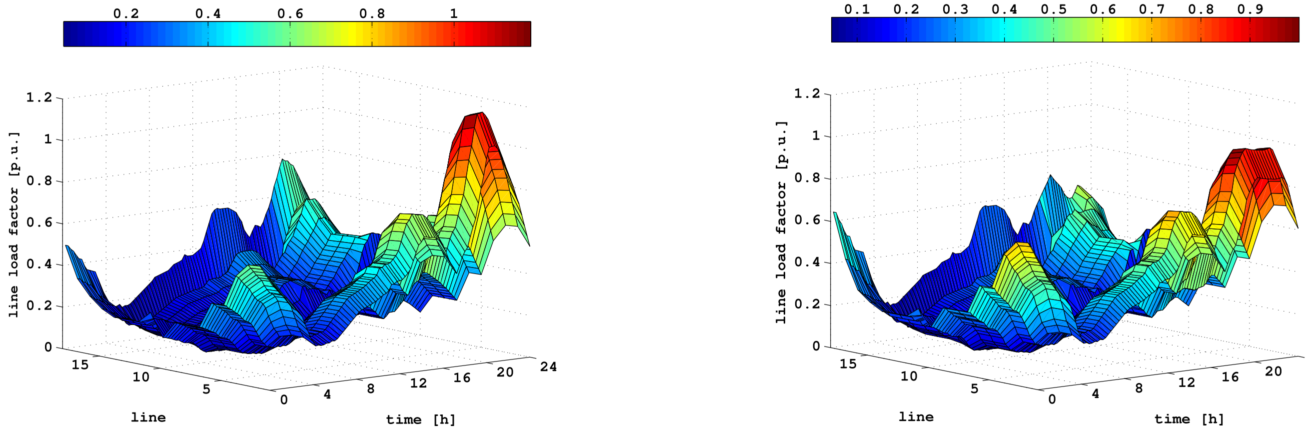

(a) (b)

Fig. 7. Comparison of line load factors of one day of simulation. (a) Smart charge algorithm OFF. (b) Smart charge algorithm ON.

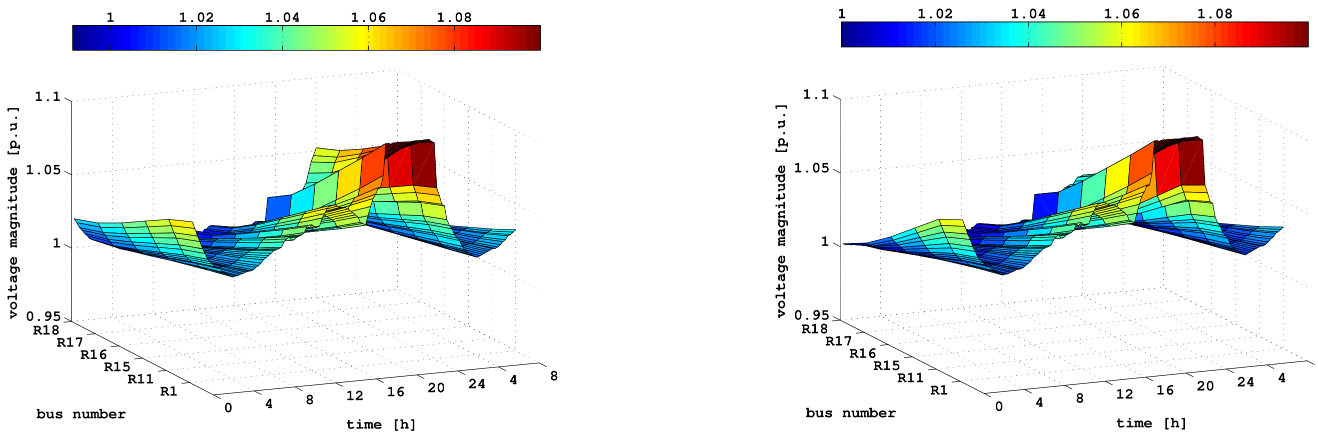

(a) (b)

Fig. 8. Comparison of voltage profiles of one day of simulation for load buses and bus R1. (a) Smart charge algorithm OFF. (b) Smart charge algorithm ON.

TABLE II
OVERALL SIMULATION RESULTS OF 300 PEVS RECHARGE OVER FIVE YEAR

Average recharge time	Average number of full capacity charge per year
[% h/year]	
22.9%	107

on average for about 22.9% of time during a year and performs, on average, 107 full charges (i.e., from fully depleted to fully charged). It is also worth mentioning that for every run the maximum number of variables in the second optimization level is 9600 whereas in the first optimization level the maximum total number of variables is 10 848, which corresponds to 32 consecutive runs of the OPF algorithm, each run optimizing 339 variables. The first number (i.e., 9600) derives from considering a total number of 300 PEVs simultaneously recharging with an 8 h recharge time. The second one (i.e., 10 848) derives from considering the variables involved in the OPF of the network (i.e., 39), to which a maximum number of 300 "generators" has been added. Power production of these generators (indeed, each of them is a load, but is treated as a generator with a specific cost function

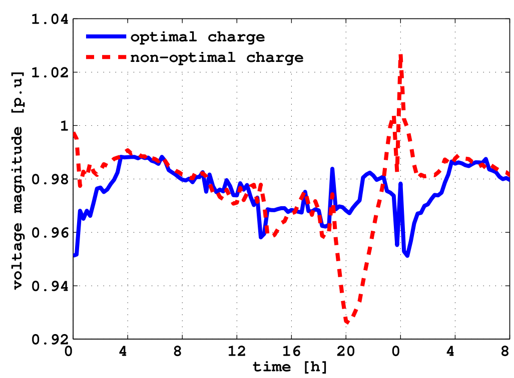

Fig. 9. Voltage profiles of bus R18: optimal recharge (solid blue line) and nonoptimal recharge (dotted red line).

as described in Section II-A) is minimized by the OPF. The heaviest condition occurs when 300 PEVs recharge simultaneously with an 8 h recharge time (i.e., a 32-quarter-of-an-hour time horizon).

V. CONCLUSION

In this paper, a two-stage margin-based algorithm for optimal PEV recharge is proposed and described. A proof of concept of the algorithm operation is provided by a one-day simulation. The scenario depicts a residential feeder with high PEV penetration (300 PEVs). The vehicles connection times and energy requests are defined according to data retrieved from mobility surveys and used for setting up a Monte Carlo simulation framework.

The proposed algorithm optimally exploits the power margin of the network while respecting end-user desired performances. Results show that the algorithm behaves as expected. In fact, it completes the recharge without trespassing cables capacity and bus voltage limits. This results in a peak shift and a "valley fill" of the feeder load curve, thus achieving a more regular voltage profile.

The obtained recharge schedules utilize the calculated margin according to a simple objective function which is not related to energy prices or other external signals. Different recharge profiles can be obtained modifying the objective function. This would lead to a different utilization of the available power margin without causing technical problems to the network.

As mentioned in Section III, future works will investigate the algorithm long-term average performances and its sensitivity to forecast uncertainties with Monte Carlo simulations. Another issue of interest might be the simulation of different objective functions in order to compare the resulting recharge schedules and assess their effects on the upstream power system.

REFERENCES

[1] J. Kim and H.-I. Park, "Policy directions for the smart grid in Korea," *IEEE Power Energy Mag.*, vol. 9, no. 1, pp. 40–49, Jan./Feb. 2011.

[2] M. Munson, G. Jaskulski, and C. Thomas, "If these walls could think," *IEEE Power Energy Mag.*, vol. 9, no. 1, pp. 50–55, Jan./Feb. 2011.

[3] S. Grillo, M. Marinelli, S. Massucco, and F. Silvestro, "Optimal management strategy of a battery-based storage system to improve renewable energy integration in distribution networks," *IEEE Trans. Smart Grid*, vol. 3, no. 2, pp. 950–958, Jun. 2012.

[4] F. Li, N. P. Padhy, J. Wang, and B. Kuri, "Cost-benefit reflective distribution charging methodology," *IEEE Trans. Power Syst.*, vol. 23, no. 1, pp. 58–64, Feb. 2008.

[5] F. Alvarez and H. Rudnick, "Impact of energy efficiency incentives on electricity distribution companies," *IEEE Trans. Power Syst.*, vol. 25, no. 4, pp. 1865–1872, Nov. 2010.

[6] R. Belhomme, R. Cerero, G. Valtorta, and P. Eyrolles, "The ADDRESS project: Developing active demand in smart power systems integrating renewables," in *Proc. IEEE Power Energy Soc. Gen. Meeting*, San Diego, CA, USA, Jul. 2011, pp. 1–8.

[7] M. D. Galus, S. Art, and G. Andersson, "A hierarchical, distributed PEV charging control in low voltage distribution grids to ensure network security," in *Proc. IEEE Power Energy Soc. Gen. Meeting*, San Diego, CA, USA, Jul. 2012, pp. 1–8.

[8] S. Babaei, D. Steen, L. A. Tuan, O. Carlson, and L. Bertling, "Effects of plug-in electric vehicles on distribution systems: A real case of Gothenburg," in *Proc. IEEE PES Innov. Smart Grid Technol. Conf. Europe (ISGT Europe)*, Gothenburg, Sweden, Oct. 2010, pp. 1–8.

[9] Z. Darabi and M. Ferdowsi, "Aggregated impact of plug-in hybrid electric vehicles on electricity demand profile," *IEEE Trans. Sustain. Energy*, vol. 2, no. 4, pp. 501–508, Oct. 2011.

[10] A. Andreotti, G. Carpinelli, F. Mottola, and D. Proto, "A review of single-objective optimization models for plug-in vehicles operation in smart grids part I: Theoretical aspects," in *Proc. IEEE Power Energy Soc. Gen. Meeting*, San Diego, CA, USA, Jul. 2012, pp. 1–8.

[11] A. Andreotti, G. Carpinelli, F. Mottola, and D. Proto, "A review of single-objective optimization models for plug-in vehicles operation in smart grids part II: Numerical applications to vehicles fleets," in *Proc. IEEE Power Energy Soc. Gen. Meeting*, San Diego, CA, USA, Jul. 2012, pp. 1–8.

[12] A. Ashtari, E. Bibeau, S. Shahidinejad, and T. Molinski, "PEV charging profile prediction and analysis based on vehicle usage data," *IEEE Trans. Smart Grid*, vol. 3, no. 1, pp. 341–350, Mar. 2012.

[13] I. Sharma, C. A. Cañizares, and K. Bhattacharya, "Modeling and impacts of smart charging PEVs in residential distribution systems," in *Proc. IEEE Power Energy Soc. Gen. Meeting*, San Diego, CA, USA, Jul. 2012, pp. 1–8.

[14] S. Paudyal, C. A. Cañizares, and K. Bhattacharya, "Optimal operation of distribution feeders in smart grids," *IEEE Trans. Ind. Electron.*, vol. 58, no. 10, pp. 4495–4503, Oct. 2011.

[15] L. Kelly, A. Rowe, and P. Wild, "Analyzing the impacts of plug-in electric vehicles on distribution networks in British Columbia," in *Proc. Elect. Power Energy Conf. (EPEC)*, Montreal, QC, Canada, Oct. 2009, pp. 1–6.

[16] M. A. Ortega-Vazquez, F. Bouffard, and V. Silva, "Electric vehicle aggregator/system operator coordination for charging scheduling and services procurement," *IEEE Trans. Power Syst.*, vol. 28, no. 2, pp. 1806–1815, May 2013.

[17] Z. Ma, D. S. Callaway, and I. A. Hiskens, "Decentralized charging control of large populations of plug-in electric vehicles," *IEEE Trans. Control Syst. Technol.*, vol. 21, no. 1, pp. 67–78, Jan. 2013.

[18] K. Strunz *et al.*, "Benchmark systems for network integration of renewable and distributed energy resources," CIGRÉ TF 6.04.02, Tech. Brochure 575, Apr. 2014.

[19] *Voltage Characteristics of Electricity Supplied by Public Distribution Networks*, CENELEC Standard EN 50160, 2008.

[20] A. Borghetti *et al.*, "Short-term scheduling and control of active distribution systems with high penetration of renewable resources," *IEEE Trans. Syst. J.*, vol. 4, no. 3, pp. 313–322, Sep. 2010.

[21] S. Paoletti *et al.*, "Load forecasting for active distribution networks," in *Proc. 2nd IEEE PES Int. Conf. Exhibit. Innov. Smart Grid Technol. (ISGT Europe)*, Manchester, U.K., Dec. 2011, pp. 1–6.

[22] F. Baccino *et al.*, "A methodology for evaluating PEVs hosting capacity margins in distribution grids," in *Proc. IEEE Power Energy Soc. Gen. Meeting*, San Diego, CA, USA, Jul. 2012, pp. 1–6.

[23] R. Lombardia, "Indagine regionale origine/destinazione—Regional mobility survey," Direzione Generale Infrastrutture e Mobilità, Regione Lombardia, Lombardy, Italy, Tech. Rep. 1015325, Jul. 2002, in Italian.

[24] R. D. Zimmerman, C. E. Murillo-Sánchez, and R. J. Thomas, "MATPOWER: Steady-state operations, planning, and analysis tools for power systems research and education," *IEEE Trans. Power Syst.*, vol. 26, no. 1, pp. 12–19, Feb. 2011.